Available online at www.sciencedirect.com

ScienceDirect

Procedia CIRP 41 (2016) 431 – 436

www.elsevier.com/locate/procedia

48th CIRP Conference on MANUFACTURING SYSTEMS - CIRP CMS 2015

Neural networks tool condition monitoring in single-point dressing operations

Doriana M. D'Addona[a,]*, Davide Matarazzo[a], Paulo R. de Aguiar[b], Eduardo C. Bianchi[b], Cesar H.R. Martins[b]

[a] *Fraunhofer Joint Laboratory of Excellence on Advanced Production Technology (Fh-J_LEAPT Naples)*
Dept. of Chemical, Material and Industrial Production Engineering, University of Naples Federico II, Piazzale Tecchio 80, 80125 Naples, Italy
[b] *Univ. Estadual Paulista – UNESP – Faculty of Engineering, Department of Electrical Engineering, 17033-360, Bauru, SP, Brazil*

* Corresponding author. Tel.: +39 081 2399231; fax: +39 081 7682362. *E-mail address:* daddona@unina.it

Abstract

Cognitive modeling of tool wear progress is employed to obtain a dependable trend of tool wear curves for optimal utilization of tool life and productivity improvement, while preserving the surface integrity of the ground parts. This paper describes a method to characterize the dresser wear condition utilizing vibration signals by applying a cognitive paradigm, such as Artificial Neural Networks (ANNs). Dressing tests with a single-point dresser were performed in a surface grinding machine and tool wear measurements taken along the experiments. The results show that ANN processing offers an effective method for the monitoring of grinding wheel wear based on vibration signal analysis.

Peer-review under responsibility of the scientific committee of 48th CIRP Conference on MANUFACTURING SYSTEMS - CIRP CMS 2015

Keywords: Dressing; Vibration signal; Tool wear; Artificial neural networks

1. Introduction

Many factors such as workpiece, machine, grinding wheel and process settings directly influence the grinding process making it highly difficult to control. The grinding wheel is a distinctive factor, among others, differentiating the grinding process from other cutting processes. The wheel topography and conditions under which it is prepared have a considerable influence upon the grinding performance [1].

An important role in the surface roughness is played by the grinding wheel. The online monitoring of the grinding wheel conditions is fundamental to achieve the best performance during the grinding process [2].

This study aims to monitor the wear of a grinding wheel during dressing operations and to correlate it with measurable sensor signals (such as force, acoustic emission (AE), vibration, current, etc.) [3]. This procedure allows to control the tool conditions and it will be supported by using an Artificial Neural Network model (ANN) for decision making. ANN models have already been employed to predict the dressing wear of grinding operations on the basis of the measured AE signals and, furthermore, working parameters of cutting operations [4].

2. Dressing tests

According to [3], a data acquisition system was set up to allow the analysis of the dressing tool wear conditions.

The vibration sensor was attached to the dresser holder and the signal was collected at a frequency of two million samples per second, using a Yokogawa DL850 oscilloscope. At the end of the tests, the signals were processed digitally.

The type of grinding wheel and the employed dresser are explained in [3].

The process consisted of a grinding operation of 170 passes; for each pass the acquired file was identified with the coded name *"PASSm"*, with *m = 0001, …, 0170*. A few grinding passes were not considered valid for the analysis, since the operator did not handle the machine correctly for those passes. For each pass the dresser condition was

Peer-review under responsibility of the scientific committee of 48th CIRP Conference on MANUFACTURING SYSTEMS - CIRP CMS 2015
doi:10.1016/j.procir.2016.01.001

observed, until the end of the dresser life [3].

The diamond wear was evaluated by measuring the diamond tip every 20 passes in each test, using a microscope under 10-100x magnifications. The obtained images of the diamond were evaluated using Leica Application Suite software.

3. Processing of the vibration signal

From each dressing signal, the dressing pass signal needed to be extracted, since each file contained noise (end and beginning) and the dressing pass signal itself. The acquired vibration signal included tails, which were not needed for the subsequent elaborations and, rather might cause longer elaboration time and generate noise while extracting signal features. Since the sensor acquired information before that the grinding wheel felt the workpiece, the vibration signals needed a previous elaboration to cut the tails. Figure 1 shows the raw signal of PASS 0005, while Figure 2 shows the cut dressing signal without tails.

Once the tails were cut, the raw vibration signal had to be filtered out, before beginning the process to obtain signal features and parameters. The filtering process was carried out by using a low-pass filter, with cutting frequency of 10 kHz. Since the vibration sensor also delivers higher frequency components, this procedure was required. The guaranteed calibration of the sensor was up to 7 to 8 kHz.

Figures 3 - 5 show the dressing vibration signal (in blue) and the dressing filtered vibration signal (in red), respectively for the PASS 0005, 0075 and 0125.

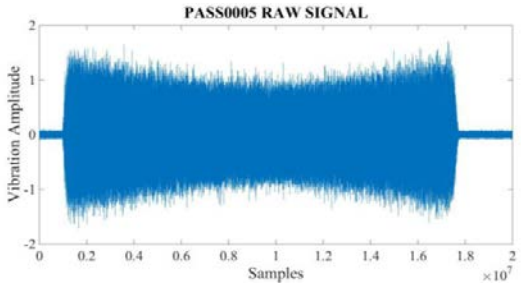

Fig. 1. PASS 0005 original raw vibration signal.

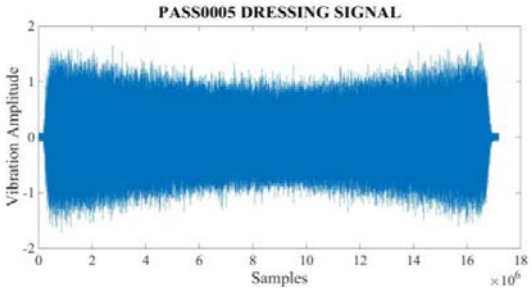

Fig. 2. PASS 0005 dressing raw vibration signal.

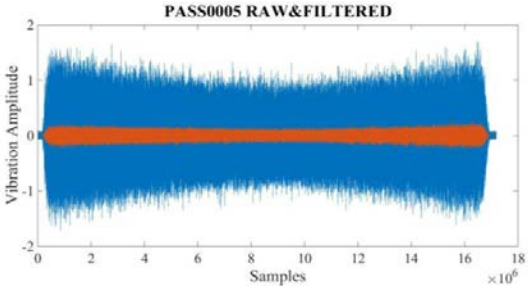

Fig. 3. PASS 0005 raw (blue) and filtered (red) signals.

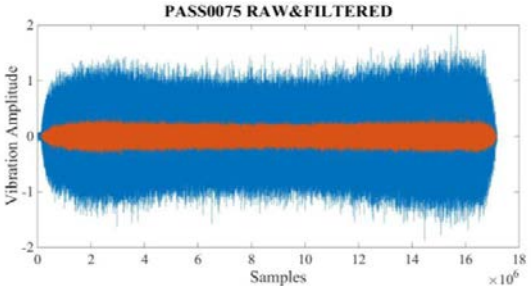

Fig. 4. PASS 0075 raw (blue) and filtered (red) signals.

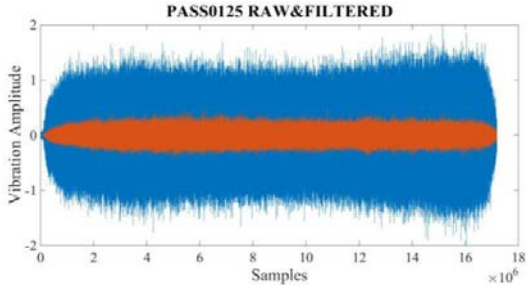

Fig. 5. PASS 0125 raw (blue) and filtered (red) signals.

4. Study of the frequencies

The frequency spectra of the filtered vibration signals for the PASS 0005, 0075 and 0125 are showed in Figures 6 - 8. The vibration signals exhibit different characteristics in the frequency domain, according to the wear condition. The other passes presented similar frequency contents.

According to the tool condition trend, the vibration signal magnitude of these curves present different features in the frequency domain It is easy to note that, in a defined range of frequencies, the vibration amplitude increases as the tool gets worn.

On the basis of the frequency spectra behavior of the vibration signals, two bands of frequencies were observed, according to the selected significant differences in magnitudes of the three tool conditions (new, half-life, and worn) were observed.

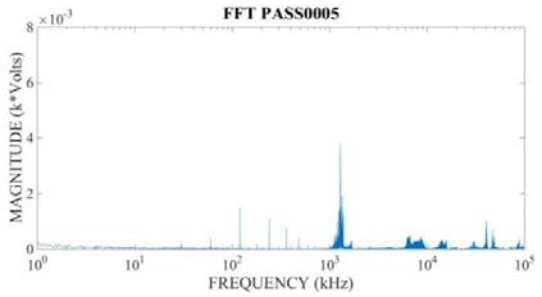

Fig. 6. PASS 0005 frequency spectra.

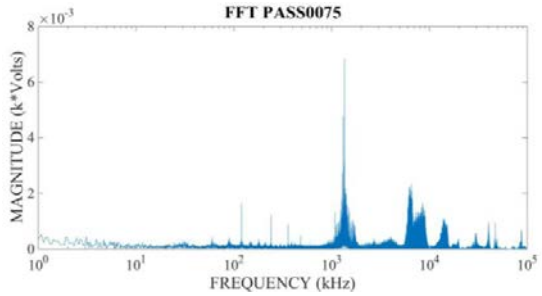

Fig. 7. PASS 0075 frequency spectra.

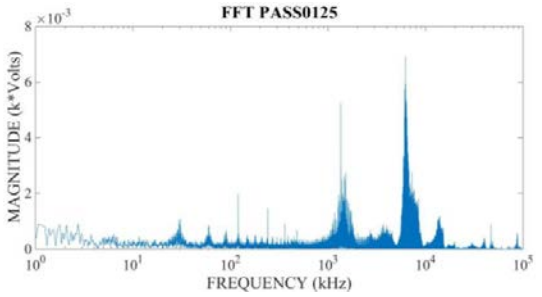

Fig. 8. PASS 0125 frequency spectra.

Figure 9 shows the vibration frequency spectra of the three selected wear conditions. The conditions were selected according to the following criterion:

1. PASS from 1 to 20: new dresser;
2. PASS from 21 to 135: half-life dresser;
3. PASS from 136: worn dresser.

For the two frequency bands considered, the mean RMS value was calculated, with reference to five passes in each wear condition. The raw vibration signal, for each frequency band, was first filtered through a first-order Butterworth band-pass filter, with a cutting frequency of 15 kHz, and the RMS values were calculated.

Figure 10 shows the RMS values, respectively, for the two different frequency bands considered, 1-2 kHz and 5-9 kHz, and for the dresser conditions: new dresser (blue line), dresser at half-life (yellow line), and worn dresser (red line).

5. Wear area results of the dressers

From the images of the diamond tips and the wear area obtained as described in [3], the mean values of wear area were calculated for the three tests performed.

Figure 11 shows the trend of the wear area, according to the grinding pass. A linear tendency in increasing wear can be observed.

6. Sensor signal feature extraction

The signal spectrum is assumed to have a specific functional form, the parameters of which are unknown. The spectral estimation problem, therefore, becomes one of estimating these unknown parameters of the spectrum model rather than the spectrum itself [5].

From each signal specimen (measurement vector), p features $\{a_1, \ldots, a_p\}$, characteristic of the spectrum model, are obtained through Linear Predictive Analysis (LPA) by applying Durbin's algorithm [6]. The details of this procedure are given in [7].

In this study, it was chosen to set $p = 4$. in Table 1 there is reported an example of the a features extracted for each vibration signal.

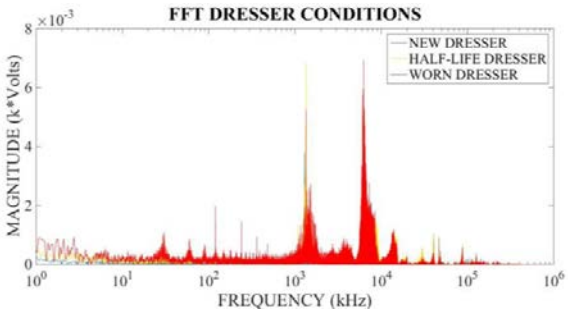

Fig. 9. Frequency of the three wear conditions.

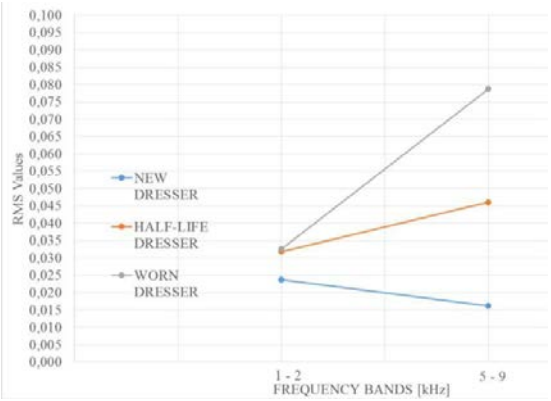

Fig. 10. RMS values for the selected frequency bands.

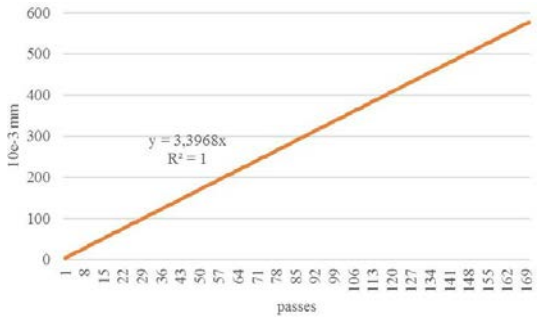

Fig. 11. Observed dressing wear trend.

7. Neural networks models

The performances of a neural network might sensibly change according to the input parameters, network function, training function, number of nodes and epochs. The features, those were extracted from every vibration signal, were then used to construct the ANN model.

7.1. Neural network input matrix

The selected parameters, which form each row vector of the input matrix, were chosen according to the characteristic features of each pass of the vibration signal.

It can be concluded that each input vector was created as follows:

1. PASS number;
2. *p* feature parameters, by setting $p = 4$ (4PARs);
3. RMS value of each PASS (calculated on each cut and filtered signal).

Each i $\{\forall\ i = 1, \ldots, n\}$ row was utilized to construct the ANN input matrix of n rows, where n $\{n = 1, \ldots, 145/165\}$ is the number of the last considered PASS (Table 2).

In order to train the ANNs, three ranges were considered to define the dresser condition (see Section 4).

To construct the input matrix, two different size were considered: the WORN DRESSER range was considered both to PASS 145 and to PASS 165.

Table 1. Sensor signal extracted features.

PASS	**Extracted features (*a*)**			
0001	3,12	-4,00	2,55	-0,67
0002	3,06	-3,91	2,52	-0,69
…	…	…	…	…
m	a_1	a_2	a_3	a_4

Table 2. ANN input matrix.

PASS	**4PARs**				**RMS**
i	$1^{st}PAR_i$	$2^{nd}PAR_i$	$3^{rd}PAR_i$	$4^{th}PAR_i$	RMS_i
i+1	$1^{st}PAR_{i+1}$	$2^{nd}PAR_{i+1}$	$3^{rd}PAR_{i+1}$	$4^{th}PAR_{i+1}$	RMS_{i+1}
…	…	…	…	…	…
n	$1^{st}PAR_n$	$2^{nd}PAR_n$	$3^{rd}PAR_n$	$4^{th}PAR_n$	RMS_n

7.2. Neural network output matrix

The ANN output is representative both of the dresser wear conditions and the Y measured dresser wear values. The ANN were trained to predict different types of output. The output has been characterized into two ways: by a single-column vector, $\{n \times 1\}$, where the column was representative of the required output, and / or a $\{n \times 2\}$ matrix, with two columns representative of the two researched output.

Firstly, the ANNs were trained to predict two outputs: a coded one, along with a prediction of the Y measured trend, secondly, to predict only the coded output and, thirdly, to predict the Y values.

In order to identify the output (actual dresser wear), the three dresser conditions were coded has follows:

1. Value "1" for the NEW DRESSER condition (Class 1);
2. Value "2" for the HALF-LIFE DRESSER condition (Class 2);
3. Value "3" for the WORN DRESSER condition (Class 3).

Tables 3 - 4 show some examples of the ANN output vectors, in particular for PASS # 0005, 0075 and 0140, with reference to the investigated output conditions.

Both the ANN output matrix and the ANN vector, will be further marked with the letter *T* when training the ANN. All the studies were conducted for a variable size dataset, by setting $n = 145$ and $n = 165$ on the basis of vibration signal passes.

7.3. Confusion Matrixes

Figure 12(a, b) show the confusion matrix for two neural network configurations, which use the 4PARs as input vector and the size data set $n = 145$ (ANN model 1) and $n = 165$ (ANN model 2), respectively.

In the matrixes, the diagonal represents the classification success carried out by the neural network, which is represented by the green colour. In those cells, the superior number represent the number of samples classified for each given class, and the inferior number represents the percentage of those samples related to the total of samples. The error of the ANN models is represented by the red cells in the matrixes and it might be considered (false positive or false negative) for each given class.

Table 3. Examples of ANN outputs for double outputs prediction.

	2 outputs ANN	
PASS #	**Tool wear class**	**Y value**
0005	1	20,3808
0075	2	258,1568
0140	3	485,7424

Table 4. Examples of ANN outputs for single output predictions.

	1 output ANN	**1 output ANN**
PASS #	**Tool wear class**	**Y value**
0005	1	20,3808
0075	2	258,1568
0140	3	485,7424

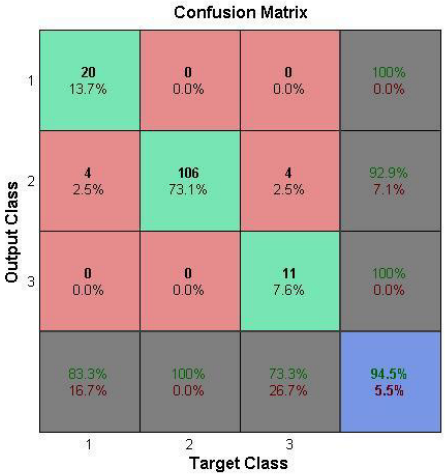

(a)

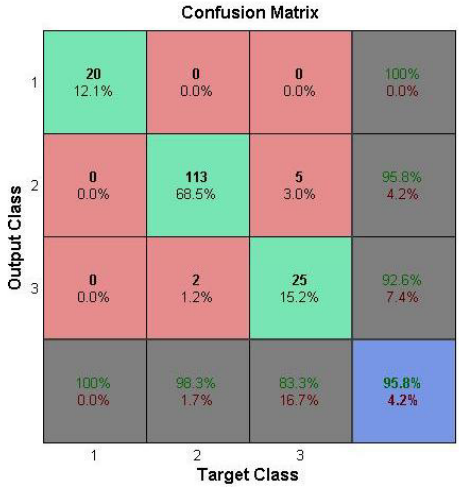

(b)

Fig. 12. Confusion matrixes for ANN model 1, (a), and model 2, (b).

The incorrectness number of each sample is represented by the superior number in each red cell, while the inferior number represents the percentage of these samples related to the total of samples. The ANN capacity to predict the output is represented in the grey columns; in those columns, the superior number of each cell is the prediction success [%], while the inferior number prediction error [%].

The Confusion matrix, for each given class, supplies the sensitivity of the ANN for each given class (grey rows), which relates to the model's ability for identifying positive results. In those cells, the superior number is the model sensitivity in percentage and the inferior number is the model sensitivity error in percentage. The total of the ANN success is represented in the blue cells, where the superior number is the percentage of model total success and the inferior number is the percentage of model total error [3].

In figure 12(a), the ANN model 1 presented an excellent predictive capacity (100%) for new and worn tool conditions (class 1 and 3, respectively), and very good predictive capacity for half-life tool condition (92.9%). The most severe wear condition was the one that showed the lowest level of sensitivity, 73.3%, due to the four dressing passes classified as half-life (class 2). The overall accuracy rate of this network was 94.5%.

In figure 12(b), for the new tool condition (class 1), the ANN model 2 presented a predictive capacity of 100% and a sensitivity of 100%. In the half-life condition (class 2), one can observe a sensitivity of 98.3%, corresponding to the occurrence of five false negative, and the predictive capacity was 95.8%. The most severe wear condition was the one that showed the lowest level of sensitivity, 83.3%, due to the five dressing passes classified as half-life. The overall accuracy rate of this network was 95.8%.

8. Implemented neural networks

In order to predict best both the coded output and the dresser wear values, it was chosen to work with Back Propagation Neural Networks (BP NN), which are particularly indicated to understand functional relationships between given inputs and outputs. To create in MATLAB R2014b a BP NN, the *newcf* (NCF) function was utilized [8, 9], according to the following code:

$$net = newcf(P', T', [S_1\, S_i], \{TF_1\, TF_2 \ldots TF_N\}); \quad (1)$$

where:

- Newcf: function to create a cascade-forward BP network;
- P': to transpose input matrix or array: R x Q1 matrix of Q1 sample R-element input vectors;
- T': to transpose target matrix or array: S_N x Q2 matrix of Q2 sample S_N-element input vectors;
- S_i: number of input and output layers: size of i^{th} layer, for N-1 layers;
- TF_N: to transfer function of the i^{th} layer.

The expression (1) returned a 3-layer cascade-forward BP network, the chosen transfer function between input layer and hidden layer was the *tangent sigmoid*, while a *linear function* was chosen as transfer function between hidden layer and output layer.

The size of the output layer varied among 1 and 2 and it depended by the type of chosen output: 1 to predict a single output (tool wear class or Y value), 2 for the double outputs ANN (tool wear class and Y value).

In order to test the performances of the *newcf* ANNs, the leave-k-out (l-k-o) method has been applied by setting $k = 1$. The method consists in creating a testing variable, by leaving out the *k-th row* of the input matrix (*TS* vector) and of the output vector / matrix (*PS* vector), then training the net with the remaining *n-k rows* and, eventually, testing the performance by comparing the ANN predicted output with the testing variable *PS*.

To have a better understanding of the ANN performances

[9], they have been also trained by using the *cascadeforwardnet* (CFN) function, which has the following MATLAB synthax:

cascadeforwardnet(hiddenSizes,trainFcn); (2)

The ANN *cascadeforwardnet* architecture differs from the ANN *newcf* architecture because of a weight connection from the input and every previous layer to the following layers and the three-layer network also has connections from the input to all three layers.

The best hidden size was chosen by trial and the net was trained with the "Training-Validation-Testing" (T-V-T) procedure, by setting the "Training" set as the 70% of the input data, the "Validation" set as the 15% and the "Test" set as the remaining 15%. The input matrix was randomly divided into these three sets [10-11].

The different ANN tested configurations are reported in Table 5.

In Table 6, the ANN best performances are showed in terms of success rate [%].

Table 5. Tested ANN configurations.

#	NET	nodes	method	%training data	k	Data set size
1	NCF	10	l-k-o	145/165 – k	1	145/165
2	CFN	50	T-V-T	70-15-15	-	145/165

Table 6. ANNs best scores.

		2 outputs ANN		1 output ANN	
#	**Data set size**	**Best class predicted**	**Success rate [%]**	**Best class predicted**	**Success rate [%]**
1	165	3	98,20%	1	99,48%
2	145	1	96,87%	-	-

9. Conclusions

This paper has addressed wear condition assessment of single-point dresser by a study of frequency content of the raw vibration signal, investigation of RMS statistics of the vibration for two frequency bands selected, and neural network models applied to classify the diamond wear as dressing operation took place.

As mentioned in literature "grinding is dressing", which is the slogan maintained in the grinding community.

The wear of the diamond in three different experiments was measured along each test. The area of wear increased as the dressing passes took place, as expected.

The study of the frequency content of the raw vibration showed a very interesting behavior for three different dresser conditions regarding the wear. While at certain frequency ranges, the vibration magnitude increased as the wear took place, this was not observed for other ranges of frequencies.

Two neural network models were developed in the search for a monitoring system capable of classifying the level of diamond wear. The models presented small errors and great success of classification. Therefore, these models may produce an acceptable result and, in turn, the ground part can yet be within project specifications.

References

[1] Nguyen T, Butler DL, Correlation of grinding wheel topography and grinding performance: A study from a ciewpoint of three-dimensional surface characterisation, J. Mater. Process. Technol., 208/1, 2008, p. 14–23.

[2] Porzycki J, "Surface-roughness model in traverse grinding," Archives Civil Mech. Eng., 5/1, 2005, p. 5–12.

[3] Martins CHR, Aguiar PR, Frech, A, Bianchi EC, Tool Condition Monitoring of Single-Point Dresser Using Acoustic Emission and Neural Networks Models, Instrumentation and Measurement, 63/3, 2014, p. 667-679.

[4] D'Addona DM, Teti R, Image data processing via neural networks for tool wear prediction, Procedia CIRP, 12, 2013, p. 252-267.

[5] Stearns SD, Hush DR, Digital Signal Analysis, Prentice Hall; 2 Sub edition, 1990.

[6] Rabiner RL,Shafer RW, Digital Signal Processing of Speech Signals. Prentice-Hall, 1978.

[7] Teti R, Buonadonna P, Round Robin on AE Monitoring of Machining. Annals of the CIRP, 48(3), 1999, p. 47–69.

[8] D'Addona DM, Matarazzo D, Sharif Ullah AMM, R Teti R, Tool Wear Control through Cognitive Paradigms, Procedia CIRP, 33, 2015, p. 221-226.

[9] D'Addona DM, Matarazzo D, Di Foggia M, Caramiello C, Iannuzzi S, Inclusion Scraps Control in Aerospace Blades Production through Cognitive Paradigms, Procedia CIRP, 33, 2015, p. 322-327.

[10] Omaima N, AL-Allaf A, Cascade-Forward vs. Function Fitting Neural Network for Improving Image Quality and Learning Time in Image Compression System, Proceedings of the World Congress on Engineering, Vol II WCE 2012, July 4 - 6, 2012, London, U.K.

[11] De Jesus O, Hagan MT, Backpropagation Algorithms for a Broad Class of Dynamic Networks, IEEE Transactions on Neural Networks, 18/1, 2007, p. 14 -27.